Accepted Manuscript

Mono- and diborylated [3]ferrocenophanes

Adelina Reichert, Michael Bolte, Hans-Wolfram Lerner, Matthias Wagner

PII: S0022-328X(13)00253-2

DOI: 10.1016/j.jorganchem.2013.03.051

Reference: JOM 17961

To appear in: *Journal of Organometallic Chemistry*

Received Date: 1 March 2013

Revised Date: 25 March 2013

Accepted Date: 26 March 2013

Please cite this article as: A. Reichert, M. Bolte, H.-W. Lerner, M. Wagner, Mono- and diborylated [3]ferrocenophanes, *Journal of Organometallic Chemistry* (2013), doi: 10.1016/j.jorganchem.2013.03.051.

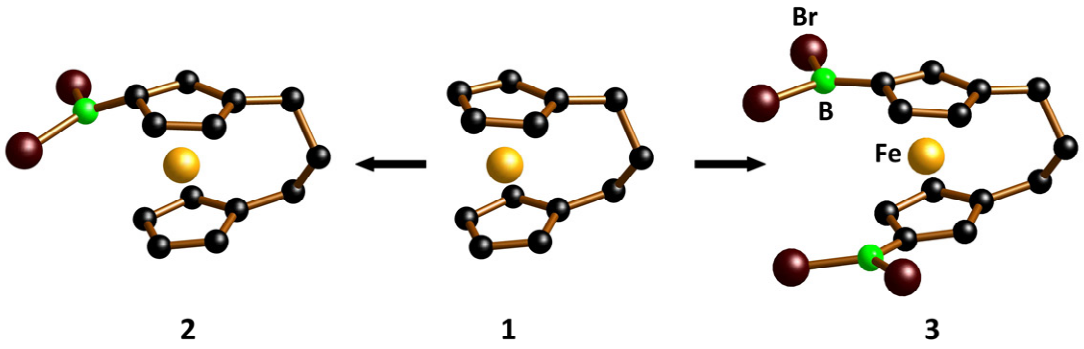

2 1 3

Synopsis:

[3]Ferrocenophane readily undergoes electrophilic borylation with BBr_3; the resulting mono- and diborylated species provide facile access to the corresponding brominated [3]ferrocenophanes, which serve as useful starting materials for Stille-coupling reactions.

Mono- and diborylated [3]ferrocenophanes

Adelina Reichert, Michael Bolte, Hans-Wolfram Lerner, Matthias Wagner*

Dedicated to Professor W. A. Herrmann on the occasion of his 65th birthday

Institut für Anorganische und Analytische Chemie, J. W. Goethe-Universität Frankfurt, Max-von-Laue-Strasse 7, D-60438 Frankfurt (Main), Germany.

Corresponding author: *Matthias.Wagner@chemie.uni-frankfurt.de*

Abstract

Treatment of [3]ferrocenophane (**1**) with 0.7 eq. or 3 eq. of BBr_3 in hexane at reflux temperature gives the corresponding dibromoboryl (**2**) or 1,1'-bis(dibromoboryl) derivative (**3**) in good yields. Compounds **2** and **3** can be transformed into the corresponding di(*tert*-butoxy)boryl (**4**, **5**) and pinacolboryl [3]ferrocenophanes (**6**, **7**). Reaction of **6** and **7** with aqueous $CuBr_2$ in MeOH/^{i}PrOH at reflux temperature leads to the formation of the mono- and 1,1'-dibrominated [3]ferrocenophanes **8** and **9**; subsequent Stille-type C−C-coupling reactions with $^{n}Bu_3SnPh$ yield mono- and 1.1'-diphenylated [3]ferrocenophanes. Treatment of **6** with $Li[AlH_4]$ in Et_2O at −78 °C provides access to the monotopic lithium trihydridoborate **12**.

Keywords: boron, [3]ferrocenophane, iron, Lewis acids, organoborane, planar chirality.

1. Introduction

Borylated ferrocenes[1] are widely applied building blocks for the preparation of ferrocenes with switchable interannular bridges,[2] redox-active poly(pyrazol-1-yl)borate ligands,[3] ferrocene-containing macrocycles,[4] multiple-decker sandwich complexes,[5] boron-bridged poly(ferrocenylene)s,[6] redox-active and planar-chiral Lewis acids,[7] and anion sensors.[8]

With respect to bonding theory, ferrocenes bearing three-coordinate boryl substituents reveal an intriguing common characteristic: In these compounds, the boryl group tends to bend out of the plane of the cyclopentadienyl ring toward the Fe(II) ion. Experimental investigations augmented by quantum-chemical calculations have led to the conclusion that the phenomenon is caused by strongly delocalized orbital interactions involving the empty p orbital at the boron atom, the *ipso*-carbon atom of the adjacent C_5H_4 ring, filled d orbitals at the iron center, and a through-space interaction with the second cyclopentadienyl ring. The degree of bending is quantified using the dip angle $\alpha^* = 180° - \alpha$, whereby α is the angle between the centroid of the C_5H_4 ring, the *ipso*-carbon atom and the boron atom. The dip angle α^* generally decreases (i) when the Lewis acidity of the boryl group decreases, (ii) when an increasing number of boryl substituents is attached to the same ferrocene backbone, and (iii) upon oxidation of the Fe(II) center to its Fe(III) state.

Given the continuing interest in ferrocenylboranes, both with regard to fundamental science and to applied chemistry, it is surprising to note that no borylated *ansa*-ferrocenes have been studied so far, even though the introduction of an interannular bridge should lead to significantly new features: (i) Its inductive effect will influence the degree of Fe···B through-space interaction, (ii) its steric requirements will influence the site selectivity of the borylation reaction, and (iii) the restricted conformational freedom of *ansa*-ferrocenes will modify the preferred supramolecular structure of ferrocenylborane-containing macromolecules or polymers.

Herein we describe a systematic investigation into the electrophilic mono- and diborylation of [3]ferrocenophane **1** (Scheme 1), the transformation of the primary products into corresponding ferrocenyl(trihydrido)borates, and the convenient synthesis of brominated [3]ferrocenophanes from borylated [3]ferrocenophanes. Brominated [3]ferrocenophanes, which are difficult to prepare by other methods, are promising platforms for the development of planar-chiral ligands[9] and liquid-crystalline materials.[10]

2. Results and discussion

*2.1. Borylation of [3]ferrocenophane **1***

We chose [3]ferrocenophane **1**[11, 12] for our borylation study, because it is comparatively easily accessible and its inert hydrocarbon bridge is compatible with the use of BBr_3 as borylation reagent (Scheme 1). Under the conditions usually applied for the selective monoborylation of parent ferrocene (0.95 eq. BBr_3, hexane, reflux temperature, 5 h), **1** gave a 4:1 mixture of the mono- and diborylated species **2** and **3**. Lowering the reaction temperature to room temperature or –78 °C with concomitantly increasing the reaction time to 12 h did not lead to the expected higher product selectivity, but, on the contrary, favored the formation of the diborylated species **3** (NMR spectroscopic control; considerable amounts of starting material **1** remained undissolved in these reaction mixtures). Working with 3 eq. of BBr_3 (hexane, reflux temperature, 5 h) yielded **2** and **3** in a stoichiometric ratio of 1:9; quantitative diborylation, however, could not be achieved, even when the amount of BBr_3 was raised to 10 eq.

--- Scheme 1 ---

These experiments lead to the following conclusions: (i) Compared to ferrocene, **1** is more prone to electrophilic borylation with BBr_3, most likely because of its electron-donating 1,3-propanediyl bridge (a similarly enhanced reactivity has also been observed for ethylferrocene[13] and 1,2,3,4,5-pentamethylferrocene[14]). (ii) At elevated temperatures, an equilibrium **2** + BBr_3 ↔ **3** + HBr leads to the observed ratio of **2**:**3** = 1:9, largely independent from the amount of BBr_3 employed (3 eq.–10 eq.). We assume that steric repulsion between the two dibromoboryl substituents, which approach each other because of the *ansa*-ferrocene structure, facilitates the proto-deborylation of **3**. Given this background, we used 0.7 eq. / 3 eq. of BBr_3 to synthesize **2** (yield: 86%) / **3** (yield: 63%; contaminated with 10% of **2**) on a preparative scale.

The ^{1}H NMR spectrum of **2** (C_6D_6) shows a multiplet for the six 1,3-propanediyl protons and four multiplets, each of them integrating 1 H, for the cyclopentadienyl protons H2'–H5'. The borylated cyclopentadienyl ring gives rise to a virtual triplet (4.12 ppm; H2) and two doublets of doublets (4.34 ppm; H4 / 4.22 ppm; H5). This signal pattern suggests that the interannular bridge is dynamic at room temperature, because otherwise two sets of signals would have to be present depending on whether CH_2-b is pointing to the same side as the BBr_2 group or to the opposite side.[15] Moreover, an inspection of the coupling constants, which possess one

larger value (2.6 Hz = $^{3}J_{HH}$) and two smaller values (1.4 Hz, 1.3 Hz = $^{4}J_{HH}$), indicates that the boryl substituent is located at the β-position relative to the 1,3-propanediyl bridge. This conclusion is further supported by the X-ray crystal structure analysis of **2** (Fig. 1) and in line with previous reports on the regioselectivity of borylation reactions of ethylferrocene, 1,1'-dibromoferrocene, and 1,1'-bis(dibromoboryl)ferrocene.[1, 13]

Compound **3** shows only three proton resonances for its two cyclopentadienyl rings with chemical shift values of 4.08 ppm (vt; H2), 4.58 ppm (dd; H4), and 4.03 ppm (dd; H5). This result points towards a highly symmetric structure (on the NMR timescale) with a dynamic three-carbon bridge and magnetically equivalent cyclopentadienyl ligands (cf. also the X-ray crystal structure analysis of **3**; Fig. 2).

The $^{11}B\{^{1}H\}$ NMR resonances of **2** and **3** appear at 41.0 ppm and 48.8 ppm, respectively, in agreement with the chemical shift values of dibromoborylferrocene (46.7 ppm) and 1,1'-bis(dibromoboryl)ferrocene (50.0 ppm).[1]

Compound **2** crystallizes as a racemic mixture in the monoclinic space group $P2_1/n$. As had already been deduced from the ^{1}H NMR spectrum of **2**, the X-ray crystal structure analysis (Fig. 1) proved the BBr_2 substituent to be located at C(3).

--- Figure 1 ---

The bond lengths and angles about the boron atom possess the same values in **2** and in its unbridged congener $FcBBr_2$ (Fc = ferrocenyl).[16] However, we note a revealingly greater degree of cyclopentadienyl–BBr_2 bending in **2** (α* = 26.1°) as compared to $FcBBr_2$ (α* = 17.7°/18.9°;[16] two crystallographically independent molecules in the asymmetric unit). The dip angle of **2** thus approaches the highest values found so far for any ferrocenylborane derivatives (e.g. $FcBH_2$: α*(calcd) = 26.5°;[17] $FcBC_{12}H_8$: α* = 25.5°;[18] $FcBC_4Ph_4$: α* = 29.4°[19]). Two reasons can be envisaged for the short contact Fe(1)···B(1) = 2.698(5) Å in compound **2**: (i) The +I effect of the hydrocarbon bridge renders the iron center more electron-rich[20] and, in turn, strengthens the Fe···B interaction. (ii) The carbon atoms C(13), C(14), and C(15) are pulled away from the boryl substituent in the *ansa*-ferrocenyl fragment as evidenced by the angle between the centroids (COG) of the two cyclopentadienyl rings and the iron atom (COG(Cp(1))−Fe(1)−COG(Cp(11)) = 169.7° (**2**) vs. 175.3°/175.9° ($FcBBr_2$)[16]). Ligand bending is consequently less hampered by unfavorable interannular steric interactions in **2** than in $FcBBr_2$.

X-ray crystallography on **3** provided conclusive evidence for the structural assignment as chiral 3,3'-bis(dibromoboryl)[3]ferrocenophane rather than as *meso*-diastereomer 3,4'-bis(dibromoboryl)[3]ferrocenophane (Scheme 1). Compound **3** crystallizes as a racemic mixture in the orthorhombic space group $Pna2_1$. Most key metrical parameters of the molecular structure of **3** are the same as in **2** (Fig. 2).

--- Figure 2 ---

The discussion can therefore be restricted to the dip angles $\alpha^* = 10.2°$ (both at C(3) and at C(13)), which possess less than half the value of the dip angle of **2**. Also in the cases of $FcBBr_2$ and $fc(BBr_2)_2$ (fc = 1,1'-ferrocenediyl), α^* decreases upon going from the mono-(17.7°/18.9°)[16] to the diborylated species (9.1°)[21], which has been attributed to the fact that the electron-donor capacity of the iron atom needs to be divided between two boron acceptors in the latter molecule.[16, 17]

With the aim to generate less air- and moisture-sensitive derivatives of **2** and **3**, the compounds were first treated with $MeOSiMe_3$ in pentane at −78 °C (Scheme 1). However, after warming to room temperature, an NMR spectroscopic investigation of the reaction mixture revealed nearly quantitative deborylation with formation of [3]ferrocenophane **1**.

Better results were obtained by adding KO^tBu to **2** and **3** in C_6H_6 at room temperature. The target molecules **4** and **5** formed as orange-colored oils, which were contaminated by **1** (in the case of **4**) and **4** (in the case of **5**). Purification by column chromatography was not an option, because both **4** and **5** are still prone to hydrolysis. The problem was finally solved by transforming **4** and **5** into the pinacol derivatives **6** and **7** (Scheme 1), which could subsequently be isolated in analytically pure form after column chromatography. In spite of numerous efforts, we found no direct way leading from **2**/**3** to **6**/**7** without having to pass **4**/**5**. Yet, this will usually pose no major inconvenience if the entire reaction sequence is carried out as a one-pot procedure.

The ^1H NMR spectrum of **6** contains the signals characteristic of the *ansa*-ferrocenyl moiety together with one resonance at 1.16 ppm (integrating 12H) for the four Bpin methyl substituents. The $^{13}C\{^1H\}$ NMR spectrum, however, shows *two* methyl resonances (24.9 ppm, 25.0 ppm) as a result of the planar-chiral structure of **6**. In line with this interpretation, the diborylated species **7** gives rise to two methyl signals both in the ^1H (1.22 ppm, 1.27 ppm; 2 × 12H) and in the $^{13}C\{^1H\}$ NMR spectrum (25.0 ppm, 25.2 ppm). The structural assignment of

6 and **7** was further confirmed by X-ray crystal structure analyses (cf. the Supporting Information for more details).

We wish to emphasize in this context that the borylation of (substituted) ferrocenes via C−H activation using pinB−Bpin and the catalytic system $[Ir(OMe)(cod)]_2$/dtbpy has been investigated by Plenio et al. (pinBH = pinacolborane; dtbpy = 4,4'-di-*tert*-butyl-2,2'-bipyridine).[22] The reactions were carried out in octane for 24 h at reflux temperature. The authors note that: (i) The reactivity of parent ferrocene is significantly lower than that of benzene, (ii) the yield of $fc(Bpin)_2$ was only 8%, even when 3 eq. of pinB−Bpin were employed (fc = 1,1'-ferrocenediyl), and (iii) electron-poor ferrocenes are more reactive than electron-rich ferrocenes. Most importantly, $fc(Me)_2$ gave only 12% of the monoborylated product and no diborylated ferrocene at all. We therefore conclude that this method most likely is no option for the preparation of borylated [3]ferrocenophanes.

2.2. Transformation of borylated into brominated [3]ferrocenophanes

Ferrocene derivatives find widespread use as (planar-chiral) ligands in coordination chemistry, but also as building blocks of thermotropic liquid crystals.[9] Another field of continuing interest is the preparation of oligoferrocenes and the detailed investigation of intramolecular electron-transfer processes in their mixed-valence states.[9] In all three cases mentioned, *ansa*-ferrocenes play important roles along with their unbridged congeners. Convenient access routes to mono- and dibrominated [3]ferrocenophanes are therefore in demand, because these compounds could serve as versatile starting materials for further transformations through, e.g., Ullmann or Pd-catalyzed C−C-coupling reactions.

The monobrominated [3]ferrocenophane **8** (Scheme 2) has previously been prepared in low yields through the mercuration of **1** with $Hg(OAc)_2$, subsequent conversion of the primary product [3]FcHg(OAc) into [3]FcHg(Cl) with LiCl and finally Hg(Cl)/Br exchange with *N*-bromosuccinimide ([3]FcH = [3]ferrocenophane).[23] Apart from the use of toxic (organo)mercury compounds, the synthesis protocol requires extended reaction times and repeated chromatographic separations.

The chiral dibrominated [3]ferrocenophane **9** (Scheme 2) is unknown. Only its *meso*-diastereomer 3,4'-dibromo[3]ferrocenophane[24] has been made accessible via the dilithiation of **1** (*n*-BuLi/TMEDA), followed by the addition of $C_2F_4Br_2$.[25] The rationale behind this synthesis approach was that the lithiated intermediate holds the lithium ions as part of a bridge spanning the two cyclopentadienyl rings, which should, in turn, place the bromine atoms on

corresponding positions of each ring.[25] However, the 3,4'-dibromo[3]ferrocenophane, isolated in 20% yield after chromatographic workup, formed as a mixture with 2,5'-dibromo[3]ferrocenophane, 2-bromo[3]ferrocenophane, and **8**.

In a recent publication, Hartwig et al. have shown that bromoarenes can readily be prepared from aryl−Bpin compounds by treatment with $CuBr_2$.[26, 27] We therefore decided to extend this approach to the transformation of the ferrocenyl−Bpin derivatives **6** and **7** to bromoferrocenes **8** and **9** (Scheme 2). Indeed, solutions of the starting materials in MeOH/^{i}PrOH provided **8** and **9** in yields of 66% and 91%, respectively, upon reaction with aqueous solutions of $CuBr_2$ at reflux temperature (Scheme 2).[28] The constitution of **9** as 3,3'-dibromo[3]ferrocenophane was confirmed by X-ray crystallography (cf. the Supporting Information for more details). The NMR spectra of **8** and **9** are according to expectations (cf. the published NMR spectra of 3,4'-dibromo[3]ferrocenophane[23]) and therefore do not merit a detailed discussion.

--- Scheme 2 ---

*2.3. Compounds **6**−**9** as starting materials for C−C-coupling and hydride-transfer reactions*

It has been reported that Pd-catalyzed cross-coupling reactions of bromoaromatics and ferrocenylboronic acids often suffer from mere deborylation as a serious side reaction.[29, 30] For example, attempts to couple $fc(B(OH)_2)_2$ and PhBr provided $fc(Ph)_2$ in yields of only 10% (toluene, 2 M aqueous Na_2CO_3, $[Pd(PPh_3)_4]$) or 60% (DME, 3 M aqueous NaOH, $[PdCl_2(dppf)]$). The yields improved to 25% or 90% when PhBr was replaced by PhI.[30] Moreover, the reaction of FcBpin with 4-bromoacetophenone under Suzuki-Miyaura conditions gave the cross-coupling product in 55% yield.[22]

In order to test the behavior of **6** and **7** in Suzuki-Miyaura reactions, we tried to couple both compounds with 4-iodotoluene, applying the reaction conditions and the catalyst system that had shown the best performance in the case of $fc(B(OH)_2)_2$ (i.e., DME, 3 M aqueous NaOH, $[PdCl_2(dppf)]$). Employing **6** as the starting material, we isolated compound **10a** in 33% yield after a reaction time of 6 d at reflux temperature (Scheme 2); the use of **7** led to the partly deborylated species **6** as the major product and was therefore of no synthetic value.

We next turned our attention to the synthetic potential of **8** and **9**. A literature report on the reaction between $fc(Br)_2$ and $PhB(OH)_2$, which affords $fc(Ph)_2$ in marginal yields of 10%,[30] led us to switch from Suzuki-Miyaura- to Stille-type protocols. Indeed, **8** and **9** can readily be transformed into **10b** and **11** upon treatment with $^{n}Bu_3SnPh$ in the presence of $[Pd(P^{t}Bu_3)_2]$

under microwave conditions (170 °C, 30 min; Scheme 2). The isolated yields were 73% and 52%, respectively. The ^{1}H NMR spectra of **10b** and **11** reveal similar signal patterns for the [3]ferrocenophane moieties as in the cases of **6**/**8** and **7**/**9**. In addition, each of the spectra contains three resonances for the phenyl rings; the overall proton integral ratios are in accord with the presence of one (**10b**) and two (**11**) phenyl substituents per molecule.

The molecular structures of **10b** and **11** have also been confirmed by X-ray crystallography (Fig. 3; cf. the Supporting Information for more details on the X-ray crystal structure analysis of **10b**). The compounds crystallize with two (**10b^{A}**, **10b^{B}**) and three (**11^{A}**, **11^{B}**, **11^{C}**) crystallographically independent molecules in the asymmetric units. The dihedral angles between the phenyl substituents and the attached cyclopentadienyl rings are comparatively small in both compounds (average values: 28° (**10b**), 13° (**11**)). For steric reasons, it can be assumed that the solid-state conformation of **11** will largely be maintained also in solution. One proton on each cyclopentadienyl ligand (i.e. H(4), H(14) in Fig. 3) should thus be influenced by the ring-current effect of the phenyl substituent residing on the other cyclopentadienyl ligand. Similar arguments hold for compound **10b**. Indeed, we find one unusually upfield-shifted resonance both in the ^{1}H NMR spectrum of **10b** (3.42 ppm) and **11** (3.91 ppm). Related ring-current effects have also been described for FcPh and fc(Ph)$_2$. They are, however, less pronounced as a result of cyclopentadienyl spinning.[31]

--- Figure 3 ---

Recently, we have shown that ferrocenylboronic acids and boronic acid esters are excellent precursors for the preparation of lithium ferrocenyl(trihydrido)borate salts.[32] As an example, the ditopic borate **A** is shown in Fig. 4. The so far most important applications of **A** have been (i) its polymerization to the boron-bridged poly(ferrocenylene) **B**[32] through Me_3SiCl-induced condensation reactions and (ii) the synthesis of oligonuclear transition-metal complexes like **C**[33] (Fig. 4).

--- Figure 4 ---

In both cases it would be desirable to possess also **A**-type [3]ferrocenophanes in order to be able (i) to influence the tertiary structure of polymers **B** by restricting the conformational freedom of certain repeat units or (ii) to promote metal−metal interactions in **C**-type aggregates by forcing the peripheral complex fragments into closer proximity. For an optimization of the experimental conditions, we first studied the reaction of **6** with Li[AlH_4] and finally isolated the target [3]ferrocenophane **12** in excellent yields (Scheme 3). The ^{11}B NMR spectrum of **12** is characterized by a quartet at −28.7 ppm ($^{1}J_{BH}$ = 77 Hz), which nicely

fits to the corresponding data of Li[$FcBH_3$] (−30.6 ppm; $^1J_{BH}$ = 77 Hz)[34]. In the ^{1}H NMR spectrum, the BH_3 protons of **12** give rise to a 1:1:1:1 quartet at 0.81 ppm (Li[$FcBH_3$]: 0.86 ppm)[34]. Moreover, we found that **12** still contained approximately 0.5 eq. of (most likely Li^+-coordinated) Et_2O even though the sample had been stored under dynamic vacuum for 12 h.

--- Scheme 3 ---

Single crystals were grown in the presence of 12-crown-4; the molecular structure of the adduct **12**·(12-c-4) is shown in Fig. 5. The Li^+ ion coordinates not only to the crown-ether molecule, but also to hydrogen atoms of the trihydridoborate fragment. A more detailed discussion of the crystal structure is precluded by the fact that the contact ion pair is located on a crystallographic mirror plane which results in severe disorder not only of the 1,3-propanediyl bridge, but also of the crown-ether ligand.

The reaction protocol, that had worked faithfully in the case of **6**, failed, however, when applied to the diborylated [3]ferrocenophane **7**. According to NMR spectroscopy, the product mixture contained only a small amount of the target **A**-type *ansa*-ferrocene. Instead, we obtained mainly **12**, Li[BH_4], and a mixed [3]ferrocenophane bearing one Bpin and one trihydridoborate substituent.

3. Conclusion

Treatment of [3]ferrocenophane (**1**) with BBr_3 in hexane at reflux temperature provides access to mono- (**2**) and diborylated [3]ferrocenophanes (**3**). The electrophilic substitution reaction proceeds more readily than in the case of pristine ferrocene, most likely because of the positive inductive effect of the 1,3-propanediyl bridge. Diborylation thus already occurs as a side reaction of the monoborylation process even when only 0.95 eq. of BBr_3 are used. The first BBr_2 substituent is selectively introduced into the β-position relative to the interannular bridge. The second BBr_2 substituent gets attached to the second cyclopentadienyl ring, again at the β-position and at the maximum distance to the first BBr_2 group that is possible under these prerequisites. Compound **3** consequently forms as racemic mixture (*rac*-**3**) rather than as *meso*-diastereomer. Most likely due to steric congestion, diborylation of **1** was never quantitative, even in the presence of 10 eq. of BBr_3. We therefore assume that the second borylation step is not irreversible but part of an equilibrium system.

The primary BBr_2 products **2** and **3** can be converted into the corresponding pinacolboryl derivatives **6** and **7**, which are readily obtained in analytically pure form by column

chromatography. Reaction of **6** and **7** with $CuBr_2$ provides the brominated [3]ferrocenophanes **8** and *rac*-**9** in good yields. Compounds **8** and *rac*-**9** are highly useful starting materials for the preparation of more complex [3]ferrocenophanes through Stille-type C−C-coupling reactions. The synthesis approach to *rac*-**9** via the electrophilic borylation of **1** is conceptually unique, because other methods providing dibrominated [3]ferrocenophanes via dilithiation/bromination protocols have the inherent disadvantage that they lead to *meso*-**9** and thus cannot be used as starting materials for chiral [3]ferrocenophane derivatives.

4. Experimental

4.1. General Considerations

Unless otherwise specified, all reactions and manipulations were carried out under dry nitrogen or argon with carefully dried and degassed solvents, flame-dried glassware, and Schlenk or glove-box techniques. Hexane, C_6H_6, C_6D_6, Et_2O, THF, THF-d_8 were dried over Na/benzophenone and distilled prior to use. Column chromatography was performed by using silica gel 60 (Macherey–Nagel). 1D and 2D NMR spectra were recorded on Bruker AM 250, Avance 300, or Avance 400 spectrometers at room temperature. Chemical shifts are referenced to (residual) solvent signals ($^1H/^{13}C\{^1H\}$; C_6D_6: 7.15/128.0; THF-d_8: 1.72/25.3) or external $BF_3{\cdot}Et_2O$ (^{11}B, $^{11}B\{^1H\}$). *J* values are given in Hz. Abbreviations: s = singlet, dd = doublet of doublets, vt = virtual triplet, q = quartet, m = multiplet, n.r. = not resolved multiplet, Cp = cyclopentadienyl. Mass spectra were recorded with a PerSeptive Biosystems Mariner Biospectrometry Workstation spectrometer. Combustion analyses were performed by the Microanalytical Laboratory of the Goethe-University Frankfurt. [3]Ferrocenophane was synthesized according to literature procedures.[11, 12] KO^{t}Bu was sublimed at 260 °C and stored in a glove box. Pinacol was recrystallized from dry C_6H_6 and stored in a glove box. All other chemicals are commercially available and were used as received.

*4.2. Synthesis of **2***

Neat BBr_3 (0.21 mL, 0.55 g, 2.2 mmol) was added at room temperature via syringe to a stirred clear solution of **1** (0.700 g, 3.10 mmol) in hexane (40 mL), whereupon an orange precipitate formed. Upon heating to reflux temperature, the precipitate redissolved within minutes. After the solution had been kept at reflux temperature for 5 h, small amounts of a greenish insoluble material were removed by filtration using a Schlenk frit while the mixture was still hot. The crystallization of the product from the filtrate started already at room temperature and was completed by storing the vessel at –30 °C overnight. The crystals obtained were suitable for X-ray crystallography. Yield: 0.747 g (86%). ^1H NMR (300.0 MHz, C_6D_6): δ 4.34 (dd, $^3J_{HH}$ = 2.6 Hz, $^4J_{HH}$ = 1.3 Hz, 1H; Cp-H4), 4.24 (m, 1H; Cp-H3□/4□), 4.22 (dd, $^3J_{HH}$ = 2.6 Hz, $^4J_{HH}$ = 1.4 Hz, 1H; Cp-H5), 4.12 (vt, 1H; Cp-H2), 3.85 (m, 1H; Cp-H3□/4□), 3.63, 3.55 (2 × m, 2 × 1H; Cp-H2□/5□), 1.63–1.22 (m, 6H; CH_2); $^{11}B\{^1H\}$ NMR (96.3 MHz, C_6D_6): δ 41.0 ($h_{1/2}$

= 120 Hz); $^{13}C\{^{1}H\}$ NMR (75.4 MHz, C_6D_6): δ 96.9 (Cp-C1), 89.6 (Cp-C1□), 81.2 (Cp-C5), 78.9 (Cp-C2), 78.6 (Cp-C3□/4□), 78.4 (Cp-C4), ≈ 76* (Cp-C3), 72.9, 72.0 (2 × Cp-C2□/5□), 71.0 (Cp-C3□/4□), 34.5 (CH_2-b), 23.9 (CH_2-a), 23.5 (CH_2-a'). *This resonance was not observed in the $^{13}C\{^{1}H\}$ NMR spectrum; its chemical shift value was taken from the cross peaks in an HMBC spectrum. Anal. Calcd (%) for $C_{13}H_{13}BBr_2Fe$ (395.71): C 39.46, H 3.31. Found: C 39.27, H 3.42.

*4.3. Synthesis of **3***

Neat BBr_3 (1.02 mL, 2.65 g, 10.6 mmol) was added at room temperature via syringe to a stirred clear solution of **1** (0.800 g, 3.54 mmol) in hexane (40 mL), whereupon an orange precipitate formed. Upon heating to reflux temperature, the precipitate redissolved within minutes. After the solution had been kept at reflux temperature for 5 h, small amounts of a greenish insoluble material were removed by filtration using a Schlenk frit while the mixture was still hot. X-ray quality crystals of **3** grew together with crystals of **2** upon storage of the filtrate at –30 °C overnight. The relative amounts **3**:**2** = 9:1 were determined by ^{1}H NMR spectroscopy. Yield of **3**: 1.27 g (63%). ^{1}H NMR (300.0 MHz, C_6D_6): δ 4.58 (dd, $^{3}J_{HH}$ = 2.6 Hz, $^{4}J_{HH}$ = 1.3 Hz, 2H; Cp-H4), 4.08 (vt, 2H; Cp-H2), 4.03 (dd, $^{3}J_{HH}$ = 2.6 Hz, $^{4}J_{HH}$ = 1.4 Hz, 2H; Cp-H5), 1.39–1.21 (m, 6H; CH_2); $^{11}B\{^{1}H\}$ NMR (96.3 MHz, C_6D_6): δ 48.8 ($h_{1/2}$ = 220 Hz); $^{13}C\{^{1}H\}$ NMR (75.4 MHz, C_6D_6): δ 98.1 (Cp-C1), 81.7 (Cp-C4), 79.5 (Cp-C2), 79.3 (Cp-C5), ≈ 76* (Cp-C3), 33.6 (CH_2-b), 23.4 (CH_2-a). *This resonance was not observed in the $^{13}C\{^{1}H\}$ NMR spectrum; its chemical shift value was taken from the cross peaks in an HMBC spectrum. Anal. Calcd (%) for $C_{13}H_{12}B_2Br_4Fe$ (565.34): C 27.62, H 2.14. Found: C 27.64, H 2.24. *Note*: The combustion analysis was performed on manually selected crystals.

*4.4. Synthesis of **4***

Neat solid KO^{t}Bu (0.355 g, 3.16 mmol) was added at room temperature to a solution of **2** (0.626 g, 1.58 mmol) in C_6H_6 (25 mL). The reaction mixture was stirred overnight, the precipitate (KBr) was collected on a frit (G4), and washed with C_6H_6 (2 × 5 mL). The filtrate was evaporated in vacuo to obtain an orange oil which consisted of a mixture of **4** and deborylated [3]ferrocenophane **1** in a stoichiometric ratio of 3:1 (^{1}H NMR spectroscopic control). Yield of **4**: 0.452 g (75%). ^{1}H NMR (400.1 MHz, C_6D_6): δ 4.48 (vt, 1H; Cp-H2),

4.43 (dd, $^{3}J_{HH}$ = 2.3 Hz, $^{4}J_{HH}$ = 1.4 Hz, 1H; Cp-H4), 4.11, 4.08 (2 × m, 2 × 1H; C_5H_4), 4.07 (dd, $^{3}J_{HH}$ = 2.3 Hz, $^{4}J_{HH}$ = 1.5 Hz, 1H; Cp-H5), 4.02, 3.82 (2 × m, 2 × 1H; C_5H_4), 1.84–1.74 (m, 6H; CH_2), 1.44 (s, 18H; CH_3); $^{11}B\{^{1}H\}$ NMR (96.3 MHz, C_6D_6): δ 27.2 ($h_{1/2}$ = 190 Hz); $^{13}C\{^{1}H\}$ NMR (100.6 MHz, C_6D_6): δ 88.5 (Cp-C1), 85.6 (Cp-C1'), 78.0 (Cp-C2), 76.4 (Cp-C4), 73.4 (Cp-C5), 72.6 (CCH_3), 71.0, 70.3, 69.6, 69.1 (C_5H_4), ≈ 67* (Cp-C3), 35.3 (CH_2-b), 31.0 (CH_3), 24.9, 24.8 (CH_2-a,a'). *This resonance was not observed in the $^{13}C\{^{1}H\}$ NMR spectrum; its chemical shift value was taken from the cross peaks in an HMBC spectrum.

*4.5. Synthesis of **5***

Neat solid KO^{t}Bu (0.783 g, 6.98 mmol) was added at room temperature to a solution of a 9:1 mixture of **3** and **2** (1.021 g) in C_6H_6 (30 mL). The reaction mixture was stirred overnight, the precipitate (KBr) was collected on a frit (G4), and washed with C_6H_6 (2 × 5 mL). The filtrate was evaporated in vacuo to obtain an orange oil which consisted of a mixture of **5** and **4** in a stoichiometric ratio of 4:1 (^{1}H NMR spectroscopic control). Yield of the 1:4 mixture of **4** and **5**: 0.97 g. ^{1}H NMR (400.1 MHz, C_6D_6): δ 4.42 (dd, $^{3}J_{HH}$ = 2.2 Hz, $^{4}J_{HH}$ = 1.4 Hz, 2H; Cp-H4), 4.36 (vt, 2H; Cp-H2), 4.23 (dd, $^{3}J_{HH}$ = 2.2 Hz, $^{4}J_{HH}$ = 1.5 Hz, 2H; Cp-H5), 1.87–1.76 (m, 6H; CH_2), 1.47 (s, 36H; CH_3); $^{11}B\{^{1}H\}$ NMR (96.3 MHz, C_6D_6): δ 28.4 ($h_{1/2}$ = 390 Hz); $^{13}C\{^{1}H\}$ NMR (100.6 MHz, C_6D_6): δ 88.5 (Cp-C1), 78.1 (Cp-C2), 77.3 (Cp-C4), 73.0 (Cp-C5), 72.7 (CCH_3), ≈ 70* (Cp-C3), 35.1 (CH_2-b), 31.2 (CH_3), 24.9 (CH_2-a). *This resonance was not observed in the $^{13}C\{^{1}H\}$ NMR spectrum; its chemical shift value was taken from the cross peaks in an HMBC spectrum.

*4.6. Synthesis of **6***

Neat pinacol (0.154 g, 1.30 mmol) was added at room temperature to **4** (0.603 g; contaminated with 25% of **1**) in THF (30 mL) and the resulting clear orange solution was stirred for 24 h. All volatiles were removed under reduced pressure and the residue was treated with Et_2O (30 mL) and H_2O (20 mL). The ethereal phase was separated using a separation funnel and the aqueous phase was extracted with Et_2O (2 × 10 mL). The combined organic phases were washed with brine and dried over anhydrous $MgSO_4$. After filtration, the filtrate was evaporated to dryness in vacuo and the crude product was purified by column chromatography. Yield: 0.361 g of **6** and 0.070 g of **1** (which can be re-used). **6** crystallized

upon slow evaporation of a C_6H_6 solution in the form of yellow plates that were suitable for X-ray crystal structure analysis; mp = 93–95 °C. R_f = 0.42 (silica gel, hexane/EtOAc = 15:1). ^{1}H NMR (300.0 MHz, C_6D_6): δ 4.63 (dd, $^3J_{HH}$ = 2.3 Hz, $^4J_{HH}$ = 1.2 Hz, 1H; Cp-H4), 4.46 (vt, 1H; Cp-H2), 4.21, 4.15 (2 × m, 2 × 1H; Cp-H3'/4'), 4.02 (dd, $^3J_{HH}$ = 2.3 Hz, $^4J_{HH}$ = 1.3 Hz, 1H; Cp-H5), 3.98, 3.75 (2 × m, 2 × 1H; Cp-H2'/5'), 1.76–1.62 (m, 6H; CH_2), 1.16 (s, 12H; CH_3); ^{11}B{^{1}H} NMR (96.3 MHz, C_6D_6): δ 33.3 ($h_{1/2}$ = 270 Hz); ^{13}C{^{1}H} NMR (75.4 MHz, C_6D_6): δ 89.5 (Cp-C1), 85.9 (Cp-C1□), 82.9 (*C*CH_3), 75.7 (Cp-C2), 74.6 (Cp-C4), 74.0 (Cp-C5), 70.0, 69.8 (Cp-C2'/5'), 69.7, 68.7 (Cp-C3'/4'), ≈ 61* (Cp-C3), 35.1 (CH_2-b), 25.0, 24.9 (CH_3), 24.7, 24.6 (CH_2-a). *This resonance was not observed in the ^{13}C{^{1}H} NMR spectrum; its chemical shift value was taken from the cross peaks in an HMBC spectrum. ESI-MS: *m/z* (%) = 352 $[M]^+$ (100). Anal. Calcd (%) for $C_{19}H_{25}BFeO_2$ (352.05): C 64.82, H 7.16. Found: C 64.65, H 7.10.

4.7. Synthesis of ***7***

Neat pinacol (0.395 g, 3.34 mmol) was added at room temperature to a 4:1 mixture of **5** and **4** (0.970 g) in THF (30 mL). The resulting clear orange solution was stirred for 24 h, all volatiles were removed under reduced pressure, and the residue was treated with Et_2O (30 mL) and H_2O (20 mL). The ethereal phase was separated using a separation funnel and the aqueous phase was extracted with Et_2O (2 × 10 mL). The combined organic phases were washed with brine and dried over $MgSO_4$. After filtration, the filtrate was evaporated to dryness in vacuo and the crude product was purified by column chromatography. Yield: 0.258 g of **7** and 0.118 g of **6**. **7** crystallized upon slow evaporation of a C_6H_6 solution in the form of orange plates that were suitable for X-ray crystal structure analysis; mp = 172–174 °C. R_f = 0.28 (silica gel, hexane/EtOAc = 15:1). ^{1}H NMR (300.0 MHz, C_6D_6): δ 4.64 (dd, $^3J_{HH}$ = 2.3 Hz, $^4J_{HH}$ = 1.2 Hz, 2H; Cp-H4), 4.39 (vt, 2H; Cp-H2), 4.15 (dd, $^3J_{HH}$ = 2.3 Hz, $^4J_{HH}$ = 1.3 Hz, 2H; Cp-H5), 1.67–1.58 (m, 6H; CH_2), 1.27, 1.22 (2 × s, 2 × 12H; CH_3); ^{11}B{^{1}H} NMR (96.3 MHz, C_6D_6): δ 33.4 ($h_{1/2}$ = 480 Hz); ^{13}C{^{1}H} NMR (75.4 MHz, C_6D_6): δ 89.8 (Cp-C1), 82.9 (*C*CH_3), 75.8 (Cp-C4), 75.5 (Cp-C2), 74.2 (Cp-C5), 34.9 (CH_2-b), 25.2, 25.0 (CH_3), 24.5 (CH_2-a). ESI-MS: *m/z* (%) = 478 $[M]^+$ (100). Anal. Calcd (%) for $C_{25}H_{36}B_2FeO_4$ (478.01): C 62.82, H 7.59. Found: C 63.24, H 7.60.

*4.8. Synthesis of **8***

Neat **6** (0.163 g, 0.463 mmol) was dissolved in a MeOH/^{i}PrOH mixture (3:2; 10 mL) and a solution of $CuBr_2$ (0.310 g, 1.39 mmol) in deionized H_2O (5 mL) was added. The stirred reaction mixture was heated to reflux temperature for 16 h, cooled to room temperature, and extracted with $CHCl_3$ (3 × 15 mL). The combined organic phases were washed with H_2O (2 × 15 mL) and dried over anhydrous $MgSO_4$. After filtration, all volatiles were removed from the filtrate in vacuo. The crude product was purified by flash column chromatography to give **8** as a yellow solid. Yield: 0.093 g (66%); mp = 67–69 °C. R_f = 0.74 (silica gel, hexane/EtOAc = 15:1). ^{1}H NMR (250.1 MHz, C_6D_6): δ 4.25 (dd, $^{3}J_{HH}$ = 2.3 Hz, $^{4}J_{HH}$ = 1.3 Hz, 1H; Cp-H4), 4.17 (m, 1H; Cp-H3□/4□), 4.06 (vt, 2H; Cp-H2), 4.01 (m, 1H; Cp-H2□/5□), 3.83 (m, 1H; Cp-H3□/4□), 3.66 (m, 1H; Cp-H2□/5□), 3.56 (dd, $^{3}J_{HH}$ = 2.3 Hz, $^{4}J_{HH}$ = 1.5 Hz, 1H; Cp-H5), 1.65–1.46 (m, 6H; CH_2); $^{13}C\{^{1}H\}$ NMR (75.4 MHz, C_6D_6): δ 86.1 (Cp-C1□), 84.5 (Cp-C1), 78.2 (Cp-C3), 75.4 (Cp-C3□/4□), 71.7 (Cp-C2), 71.2 (Cp-C2□/5□), 70.7 (Cp-C4), 70.3 (Cp-C3□/4□), 70.1 (Cp-C2□/5□), 68.4 (Cp-C5), 35.3 (CH_2-b), 24.3, 24.3 (CH_2-a,a'). ESI-MS: *m/z* (%) = 304 $[M]^+$ (100).

*4.9. Synthesis of **9***

Neat **7** (0.220 g, 0.460 mmol) was dissolved in a MeOH/^{i}PrOH mixture (3:2; 15 mL) and a solution of $CuBr_2$ (0.617 g, 2.76 mmol) in deionized H_2O (10 mL) was added. The stirred reaction mixture was heated to reflux temperature for 16 h, cooled to room temperature, and extracted with $CHCl_3$ (3 × 20 mL). The combined organic phases were washed with H_2O (2 × 20 mL) and dried over anhydrous $MgSO_4$. After filtration, all volatiles were removed from the filtrate in vacuo to give **9** as an orange solid in pure form. Yield: 0.161 g (91%); mp = 152–154 °C. ^{1}H NMR (250.1 MHz, C_6D_6): δ 4.06 (dd, $^{3}J_{HH}$ = 2.4 Hz, $^{4}J_{HH}$ = 1.3 Hz, 2H; Cp-H4), 3.91 (vt, 2H; Cp-H2), 3.72 (dd, $^{3}J_{HH}$ = 2.4 Hz, $^{4}J_{HH}$ = 1.5 Hz, 2H; Cp-H5), 1.35–1.29 (m, 6H; CH_2); $^{13}C\{^{1}H\}$ NMR (75.4 MHz, C_6D_6): δ 85.0 (Cp-C1), 78.4 (Cp-C3), 77.4 (Cp-C4), 72.0 (Cp-C2), 69.9 (Cp-C5), 35.1 (CH_2-b), 23.8 (CH_2-a). ESI-MS: *m/z* (%) = 384 $[M]^+$ (100). Anal. Calcd (%) for $C_{13}H_{12}Br_2Fe$ (383.90): C 40.67, H 3.15. Found: C 40.63, H 3.19.

*4.10. Synthesis of **12***

A solution of Li[AlH_4] in Et_2O (1 M, 0.37 mL, 0.37 mmol) was diluted with Et_2O (5 mL) and added dropwise with stirring at –78 °C to a solution of **6** (0.130 g, 0.369 mmol) in Et_2O (15 mL). After 30 min, the mixture was allowed to warm to room temperature and stirred for another 1 h. The insolubles were removed by filtration (G4 frit) and washed with Et_2O (2 × 5 mL). The solvent was removed from the filtrate under reduced pressure and the solid residue was further dried under dynamic vacuum overnight to obtain **12**·$(Et_2O)_{0.5}$ as a yellow compound; the amount of Et_2O present in the sample after drying was determined by ^{1}H NMR spectroscopy. Yield: 0.089 g (85%). **12** crystallized from Et_2O/THF in the presence of 12-crown-4 at room temperature as crown-ether adduct **12**·(12-c-4). ^{1}H NMR (300.0 MHz, THF-d_8): δ 3.81 (m, 1H; Cp-H2□/5□), 3.77 (m, 1H; Cp-H3□/4□), 3.65 (n.r., 1H; Cp-H2), 3.63 (n.r., 1H; Cp-H4), 3.59 (m, 1H; Cp-H2□/5□), 3.57 (m, 1H; Cp-H5), 3.38 (m, 1H; Cp-H3□/4□), 1.91–1.78 (m, 6H; CH_2), 0.81 (q, $^1J_{BH}$ = 77 Hz, 3H; BH_3); ^{11}B{^{1}H} NMR (96.3 MHz, THF-d_8): δ –28.7 ($h_{1/2}$ = 12 Hz); ^{11}B NMR (96.3 MHz, THF-d_8): δ –28.7 (q, $^1J_{BH}$ = 77 Hz); ^{13}C{^{1}H} NMR (100.6 MHz, THF-d_8): δ 93.7 (q, $^1J_{BC}$ = 60 Hz; Cp-C3), 84.2 (m; Cp-C1), 82.8 (Cp-C1□), 77.4 (q, $^2J_{BC}$ = 3.5 Hz; Cp-C2), 75.5 (q, $^2J_{BC}$ = 3.5 Hz; Cp-C4), 72.8 (Cp-C3□/4□), 69.5 (Cp-C2□/5□), 69.1 (q, $^3J_{BC}$ = 2.5 Hz; Cp-C5), 67.7 (Cp-C3□/4□), 67.5 (Cp-C2□/5□), 36.0 (CH_2-b), 26.5, 26.2 (CH_2-a,a').

*4.11. Crystal structure determinations of **2**, **3**, **11**, and **12**.*

Data for **3** were collected on a STOE IPDS II two-circle diffractometer with graphite-monochromated MoK_α radiation (λ = 0.71073 Å). An empirical absorption correction with the program PLATON[35] was performed. Data for **2**, **11**, and **12** were collected on a STOE IPDS II two-circle diffractometer using a Genix Microfocus X-ray source with mirror optics and MoK_α radiation. The data of **2**, **11**, and **12** were corrected for absorption with the frame-scaling procedure contained in the X-AREA package. Equivalent reflections were averaged. The structures were solved by direct methods using the program SHELXS[36] and refined with full-matrix least-squares on F^2 using the program SHELXL-97.[37] H atoms were geometrically positioned and refined applying a riding model.

The absolute structure of **3** was determined: Flack-x-parameter = 0.06(4). The crystal of **3** was of minor quality, which explains the rather large standard deviations of the bond lengths and angles.

Compound **11** crystallized with three crystallographically independent molecules in the asymmetric unit (**11**^{A}, **11**^{B}, **11**^{C}). In one of these molecules, one methylene group is disordered over two positions with a site occupation factor of 0.787(6) for the major occupied site. The disordered atoms were anisotropically refined and the C–C bonds of the disordered atoms were restrained to be equal.

The molecule of **12** is located on a crystallographic mirror plane. As a result, the 1,3-propanediyl chain is disordered over two equally occupied positions. The crown-ether ring is also affected by the disorder and consequently its atoms show enlarged displacement ellipsoids.

CCDC reference numbers: 926726 (**2**), 926727 (**3**), 926728 (**11**) 926729 (**12**).

5. Acknowledgements

M.W. acknowledges financial support by the Beilstein Institute, Frankfurt/Main, Germany, within the research collaboration NanoBiC.

6. References

[1] (a) W. Ruf, M. Fueller, W. Siebert, J. Organomet. Chem. 64 (1974) C45–C47;
(b) T. Renk, W. Ruf, W. Siebert, J. Organomet. Chem. 120 (1976) 1–25;
(c) W. Ruf, T. Renk, W. Siebert, Z. Naturforsch. 31b (1976) 1028–1034;
(d) B. Wrackmeyer, U. Dörfler, M. Herberhold, Z. Naturforsch. 48b (1993) 121–123;
(e) A. Appel, H. Nöth, M. Schmidt, Chem. Ber. 128 (1995) 621–626.

[2] (a) F. Jäkle, T. Priermeier, M. Wagner, J. Chem. Soc., Chem. Commun. (1995) 1765–1766;
(b) F. Jäkle, M. Mattner, T. Priermeier, M. Wagner, J. Organomet. Chem. 502 (1995) 123–130;
(c) F. Jäkle, T. Priermeier, M. Wagner, Organometallics 15 (1996) 2033–2040;
(d) E. Herdtweck, F. Jäkle, G. Opromolla, M. Spiegler, M. Wagner, P. Zanello, Organometallics 15 (1996) 5524–5535;
(e) E. Herdtweck, F. Jäkle, M. Wagner, Organometallics 16 (1997) 4737–4745.

[3] (a) F. Jäkle, K. Polborn, M. Wagner, Chem. Ber. 129 (1996) 603–606;
(b) F. Fabrizi de Biani, F. Jäkle, M. Spiegler, M. Wagner, P. Zanello, Inorg. Chem. 36 (1997) 2103–2111;
(c) E. Herdtweck, F. Peters, W. Scherer, M. Wagner, Polyhedron 17 (1998) 1149–1157;
(d) S.L. Guo, F. Peters, F. Fabrizi de Biani, J.W. Bats, E. Herdtweck, P. Zanello, M. Wagner, Inorg. Chem. 40 (2001) 4928–4936;
(e) A. Haghiri Ilkhechi, M. Bolte, H.-W. Lerner, M. Wagner, J. Organomet. Chem. 690 (2005) 1971–1977.

[4] (a) L. Ding, F. Fabrizi de Biani, M. Bolte, P. Zanello, M. Wagner, Organometallics 19 (2000) 5763–5768;
(b) R.E. Dinnebier, L. Ding, K. Ma, M.A. Neumann, N. Tanpipat, F.J.J. Leusen, P.W. Stephens, M. Wagner, Organometallics 20 (2001) 5642–5647;
(c) L. Ding, K. Ma, G. Dürner, M. Bolte, F. Fabrizi de Biani, P. Zanello, M. Wagner, J. Chem. Soc., Dalton Trans. (2002) 1566–1573.

[5] (a) A. Haghiri Ilkhechi, M. Scheibitz, M. Bolte, H.–W. Lerner, M. Wagner, Polyhedron 23 (2004) 2597–2604;
(b) A. Haghiri Ilkhechi, J.M. Mercero, I. Silanes, M. Bolte, M. Scheibitz, H.-W. Lerner, J.M. Ugalde, M. Wagner, J. Am. Chem. Soc. 127 (2005) 10656–10666;

(c) L. Kaufmann, A. Haghiri Ilkhechi, H. Vitze, M. Bolte, H.-W. Lerner, M. Wagner, J. Organomet. Chem. 694 (2009) 466–472.

[6] (a) M. Fontani, F. Peters, W. Scherer, W. Wachter, M. Wagner, P. Zanello, Eur. J. Inorg. Chem. (1998) 1453–1465;

(b) M. Grosche, E. Herdtweck, F. Peters, M. Wagner, Organometallics 18 (1999) 4669–4672;

(c) R.E. Dinnebier, M. Wagner, F. Peters, K. Shankland, W.I.F. David, Z. Anorg. Allg. Chem. 626 (2000) 1400–1405;

(d) M. Scheibitz, J.W. Bats, M. Bolte, H.-W. Lerner, M. Wagner, Organometallics 23 (2004) 940–942;

(e) M. Scheibitz, J.B. Heilmann, R.F. Winter, M. Bolte, J.W. Bats, M. Wagner, Dalton Trans. (2005) 159–170;

(f) J.B. Heilmann, M. Scheibitz, Y. Qin, A. Sundararaman, F. Jäkle, T. Kretz, M. Bolte, H.-W. Lerner, M.C. Holthausen, M. Wagner, Angew. Chem. Int. Ed. 45 (2006) 920–925;

(g) M. Scheibitz, H. Li, J. Schnorr, A. Sánchez Perucha, M. Bolte, H.-W. Lerner, F. Jäkle, M. Wagner, J. Am. Chem. Soc. 131 (2009) 16319–16329;

(h) L. Kaufmann, J.-M. Breunig, H. Vitze, F. Schödel, I. Nowik, M. Pichlmaier, M. Bolte, H.-W. Lerner, R.F. Winter, R.H. Herber, M. Wagner, Dalton Trans. (2009) 2940–2950;

(i) C. Cui, J. Heilmann-Brohl, A. Sánchez Perucha, M.D. Thomson, H.G. Roskos, M. Wagner, F. Jäkle, Macromolecules 43 (2010) 5256–5261.

[7] (a) F. Jäkle, A.J. Lough, I. Manners, Chem. Commun. (1999) 453–454;

(b) K. Venkatasubbaiah, L.N. Zakharov, W.S. Kassel, A.L. Rheingold, F. Jäkle, Angew. Chem. Int. Ed. 44 (2005) 5428–5433;

(c) R. Boshra, A. Doshi, F. Jäkle, Angew. Chem. Int. Ed. 47 (2008) 1134–1137;

(d) R. Boshra, A. Doshi, F. Jäkle, Organometallics 27 (2008) 1534–1541;

(e) I.R. Morgan, A. Di Paolo, D. Vidovic, I.A. Fallis, S. Aldridge, Chem. Commun. (2009) 7288–7290;

(f) J. Chen, K. Venkatasubbaiah, T. Pakkirisamy, A. Doshi, A. Yusupov, Y. Patel, R.A. Lalancette, F. Jäkle, Chem. Eur. J. 16 (2010) 8861–8867;

(g) P. Thilagar, J. Chen, R.A. Lalancette, F. Jäkle, Organometallics 30 (2011) 6734–6741.

[8] (a) C. Dusemund, K.R.A.S. Sandanayake, S. Shinkai, J. Chem. Soc., Chem. Commun. (1995) 333–334;

(b) S. Aldridge, C. Bresner, I.A. Fallis, S.J. Coles, M.B. Hursthouse, Chem. Commun. (2002) 740–741;

(c) C. Bresner, S. Aldridge, I.A. Fallis, C. Jones, L.-L. Ooi, Angew. Chem. Int. Ed. 44 (2005) 3606–3609;

(d) C. Bresner, J.K. Day, N.D. Coombs, I.A. Fallis, S. Aldridge, S.J. Coles, M.B. Hursthouse, Dalton Trans. (2006) 3660–3667;

(e) A.E.J. Broomsgrove, D.A. Addy, C. Bresner, I.A. Fallis, A.L. Thompson, S. Aldridge, Chem. Eur. J. 14 (2008) 7525–7529.

[9] A. Togni, T. Hayashi (eds.), Ferrocenes, VCH, Weinheim, Germany, 1995.

[10] (a) O. Kadkin, C. Näther, W. Friedrichsen, J. Organomet. Chem. 649 (2002) 161–172;

(b) O.N. Kadkin, H. Han, Y.G. Galyametdinov, J. Organomet. Chem. 692 (2007) 5571–5582;

(c) O.N. Kadkin, Y.G. Galyametdinov, e-Liq. Cryst. Commun. (2007) 1–14;

(d) O.N. Kadkin, J. An, H. Han, Y.G. Galyametdinov, Eur. J. Inorg. Chem. (2008) 1682–1688;

(e) O.N. Kadkin, Yu.G. Galyametdinov, Russ. Chem. Rev. 81 (2012) 675–699.

[11] T.D. Turbitt, W.E. Watts, J. Organomet. Chem. 46 (1972) 109–117.

[12] T.-Y. Dong, S.-H. Lee, J. Organomet. Chem. 487 (1995) 77–88.

[13] B. Wrackmeyer, U. Dörfler, J. Rinck, M. Herberhold, Z. Naturforsch. 49b (1994) 1403–1406.

[14] U.D. Eckensberger, K. Kunz, M. Bolte, H.-W. Lerner, M. Wagner, Organometallics 27 (2008) 764–768.

[15] A rapidly flipping 1,3-propanediyl chain has been postulated already for the [3]ferrocenophane **1**.

(a) M. Rosenblum, A.K. Banerjee, N. Danieli, R.W. Fish, V. Schlatter, J. Am. Chem. Soc. 85 (1963) 316–324;

(b) M. Hillman, J.D. Austin, Organometallics 6 (1987) 1737–1743.

[16] A. Appel, F. Jäkle, T. Priermeier, R. Schmid, M. Wagner, Organometallics 15 (1996) 1188–1194.

[17] M. Scheibitz, M. Bolte, J.W. Bats, H.-W. Lerner, I. Nowik, R.H. Herber, A. Krapp, M. Lein, M.C. Holthausen, M. Wagner, Chem. Eur. J. 11 (2005) 584–603.

[18] L. Kaufmann, H. Vitze, M. Bolte, H.-W. Lerner, M. Wagner, Organometallics 27 (2008) 6215–6221.

[19] H. Braunschweig, I. Fernández, G. Frenking, T. Kupfer, Angew. Chem. Int. Ed. 47 (2008) 1951–1954.

[20] E. Fujita, B. Gordon, M. Hillman, A.G. Nagy, J. Organomet. Chem. 218 (1981) 105–114.

[21] B. Wrackmeyer, U. Dörfler, W. Milius, M. Herberhold, Polyhedron 14 (1995) 1425–1431.

[22] A. Datta, A. Köllhofer, H. Plenio, Chem. Commun. (2004) 1508–1509.

[23] D.R. Talham, D.O. Cowan, Organometallics 6 (1987) 932–937.

[24] Note that a different numbering scheme for the cyclopentadienyl rings has been used in this publication and in ref[25].

[25] M. Hillman, L. Matyevich, E. Fujita, U. Jagwani, J. McGowan, Organometallics 1 (1982) 1226–1229.

[26] J.M. Murphy, X. Liao, J.F. Hartwig, J. Am. Chem. Soc. 129 (2007) 15434–15435.

[27] C. Reus, N.-W. Liu, M. Bolte, H.-W. Lerner, M. Wagner, J. Org. Chem. 77 (2012) 3518–3523.

[28] Addition of ^{i}PrOH to the solvent mixture enhances the solubility of the starting materials **6** and **7** and thereby increases the yields of **8** and **9**.

[29] S. Gronowitz, A.B. Hörnfeldt, Y. Yang, in O. Chizhov (ed.) Organic Synthesis: Modern Trends, Blackwell Scientific, Oxford, 1987, p. 253.

[30] R. Knapp, M. Rehahn, J. Organomet. Chem. 452 (1993) 235–240.

[31] Y. Okada, T. Hayashi, Magn. Reson. Chem. 30 (1992) 892–897.

[32] See refs.[6d] and [6g].

[33] A. Reichert, M. Bolte, H.-W. Lerner, M. Wagner, Dalton Trans. 42 (2013) 688−694.

[34] See ref[6g].

[35] A.L. Spek, J. Appl. Crystallogr. 36 (2003) 7–13.

[36] G.M. Sheldrick, Acta Crystallogr. A46 (1990) 467–473.

[37] G.M. Sheldrick, SHELXL-97, A Program for the Refinement of Crystal Structures, University of Göttingen, Göttingen, Germany, 1997.

Scheme 1

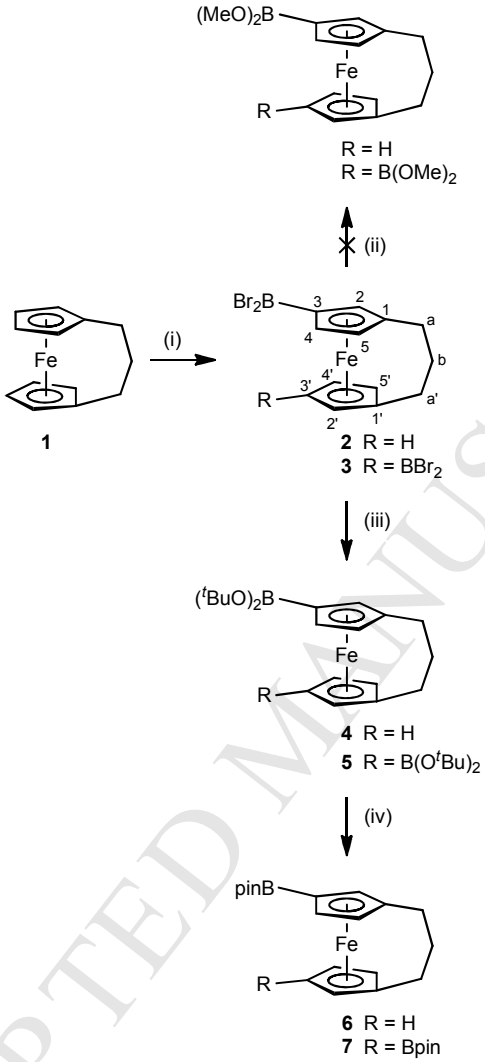

Scheme 1. Synthesis of compounds **2**–**7**. Reagents and conditions: (i) **2**: 0.7 eq. BBr_3, hexane, reflux temperature, 5 h; **3**: 3 eq. BBr_3, hexane, reflux temperature, 5 h. (ii) exc. $MeOSiMe_3$, pentane, –78 °C to room temperature, 2 h. (iii) **4**: 2 eq. KO^tBu, C_6H_6, room temperature, 12 h; **5**: 4 eq. KO^tBu, C_6H_6, room temperature, 12 h. (iv) **6**: 1 eq. pinacol, THF, room temperature, 24 h; **7**: 2 eq. pinacol, THF, room temperature, 24 h.

Scheme 2

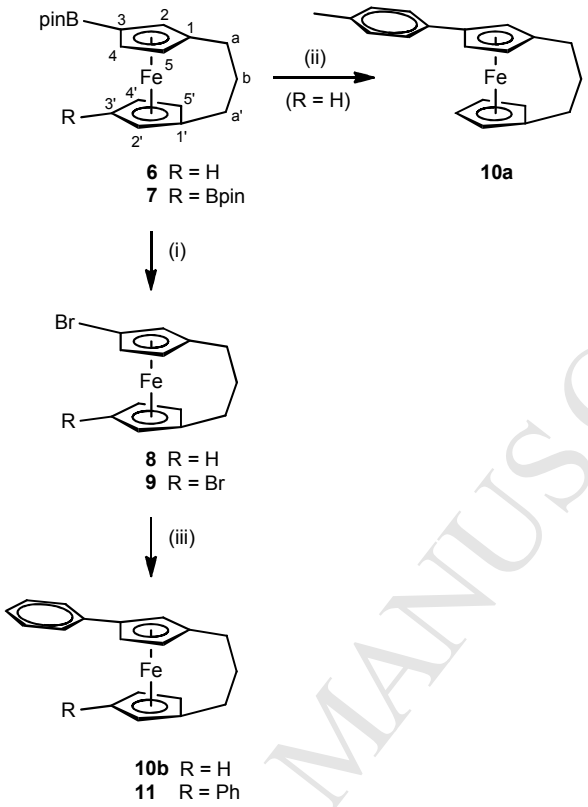

Scheme 2. Synthesis of compounds **8**–**11**. Reagents and conditions: (i) **8**: 3 eq. $CuBr_2$, H_2O/MeOH/^{i}PrOH, reflux temperature, 16 h; **9**: 6 eq. $CuBr_2$, H_2O/MeOH/^{i}PrOH, reflux temperature, 16 h. (ii) 1.5 eq. 4-Iodotoluene, 0.04 eq. [$PdCl_2$(dppf)], 3 M aqueous NaOH, DME, reflux temperature, 6 d. (iii) **10b**: 2 eq. $^{n}Bu_3SnPh$, 0.1 eq. [$Pd(P^{t}Bu_3)_2$], toluene, microwave irradiation (170 °C, 30 min); **11**: 4 eq. $^{n}Bu_3SnPh$, 0.2 eq. [$Pd(P^{t}Bu_3)_2$], toluene, microwave irradiation (170 °C, 30 min).

Scheme 3

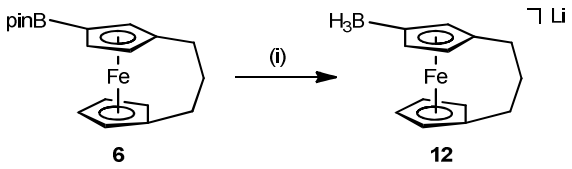

Scheme 3. Synthesis of compound **12**. Reagents and conditions: (i) 1 eq. $Li[AlH_4]$, Et_2O, –78 °C to room temperature, 1.5 h.

Figure 1

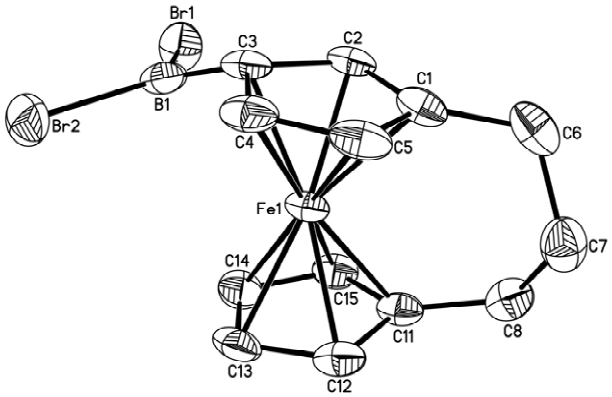

Fig. 1. Molecular structure of **2** in the solid state. Hydrogen atoms have been omitted for clarity; displacement ellipsoids are drawn at the 50% probability level. Selected bond lengths (Å), atom···atom distance (Å), bond angles (°), and dihedral angles (°): B(1)−C(3) 1.478(7), B(1)−Br(1) 1.937(5), B(1)−Br(2) 1.938(5), Fe(1)···B(1) 2.698(5); C(3)−B(1)−Br(1) 121.8(3), C(3)−B(1)−Br(2) 122.3(4), Br(1)−B(1)−Br(2) 115.6(3), COG(Cp(1))−Fe(1)−COG(Cp(11)) 169.7; Cp(C(1))//Cp(C(11)) 9.7(3), B(1)Br(1)Br(2)//Cp(C(1)) 22.4(2), C(1)Fe(1)C(11)//C(6)C(7)C(8) 57.3(3); α* 26.1. COG(Cp(X)): centroid of the cyclopentadienyl ring containing the carbon atom C(X).

Figure 2

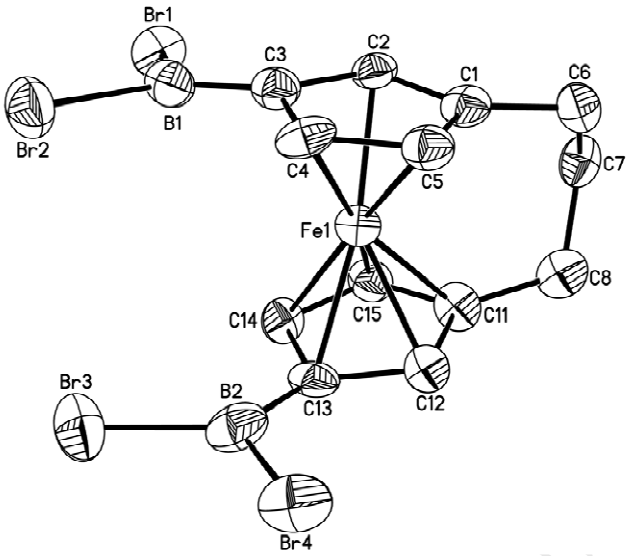

Fig. 2. Molecular structure of **3** in the solid state. Hydrogen atoms have been omitted for clarity; displacement ellipsoids are drawn at the 50% probability level. Selected bond lengths (Å), atom···atom distances (Å), bond angles (°), torsion angle (°), and dihedral angles (°): B(1)−C(3) 1.46(2), B(1)−Br(1) 1.96(2), B(1)−Br(2) 1.92(2), B(2)−C(13) 1.53(2), B(2)−Br(3) 1.92(2), B(2)−Br(4) 1.92(2); Fe(1)···B(1) 2.99(2), Fe(1)···B(2) 3.05(2); C(3)−B(1)−Br(1) 121.1(12), C(3)−B(1)−Br(2) 123.7(12), Br(1)−B(1)−Br(2) 115.2(9), C(13)−B(2)−Br(3) 121.9(12), C(13)−B(2)−Br(4) 120.9(13), Br(3)−B(2)−Br(4) 117.2(9), COG(Cp(1))−Fe(1)−COG(Cp(11)) 168.8; C(3)−COG(Cp(1))−COG(Cp(11))−C(13) –75.4; Cp(C(1))//Cp(C(11)) 11.2(6), B(1)Br(1)Br(2)//Cp(C(1)) 11.4(7), B(2)Br(3)Br(4)//Cp(C(11)) 9.0(8), C(1)Fe(1)C(11)//C(6)C(7)C(8) 59(1); α* 10.2 (at C(3)), 10.2 (at C(13)).

Figure 3

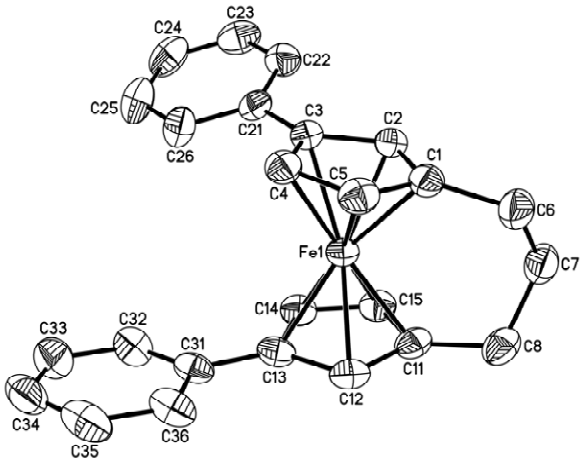

Fig. 3. Molecular structure of **11**^{A} (**11**^{B}, **11**^{C}) in the solid state. Hydrogen atoms have been omitted for clarity; displacement ellipsoids are drawn at the 50% probability level. Selected bond lengths (Å), bond angles (°), torsion angles (°), and dihedral angles (°): C(3)−C(21) 1.477(2) (1.475(2), 1.471(3)), C(13)−C(31) 1.468(3) (1.470(2), 1.469(2)); COG(Cp(1))−Fe(1)−COG(Cp(11)) 173.5 (172.9, 172.8); C(3)−COG(Cp(1))−COG(Cp(11))−C(13) 73.1 (75.7, 77.2); Cp(C(1))//Cp(C(11)) 8.8(1) (9.6(1), 9.7(1)); Cp(C(1))//Ph(C(21)) 23.0(1) (4.1(1), 21.3(1)), Cp(C(11))//Ph(C(31)) 6.9(1) (11.1(1), 9.1(1)), C(1)Fe(1)C(11)//C(6)C(7)C(8) 56.8(1) (57.3(1), 54.2(2)).

Figure 4

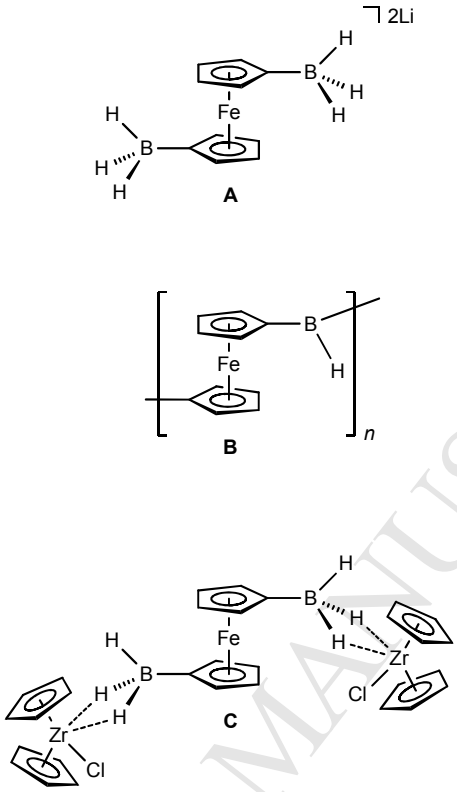

Fig. 4. The lithium ferrocenyl(trihydrido)borate **A** is a precursor for the synthesis of the boron-bridged poly(ferrocenylene) **B** and oligonuclear transition-metal complexes like **C**.

Figure 5

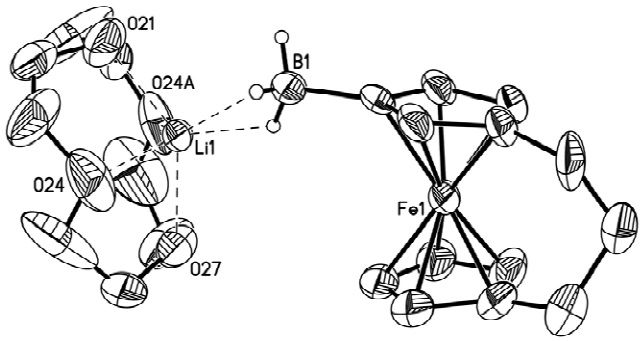

Fig. 5. Molecular structure of **12**·(12-c-4) in the solid state. Hydrogen atoms except on boron have been omitted for clarity; displacement ellipsoids are drawn at the 30% probability level. The bond lengths and bond angles are not given due to poor crystallographic data, which lead to large error margins.

Table 1

Selected Crystallographic Data and Structure Refinement for **2** and **3**.

	2	**3**
formula	$C_{13}H_{13}BBr_2Fe$	$C_{13}H_{12}B_2Br_4Fe$
fw	395.71	565.34
color, shape	orange, plate	red, plate
temp (K)	173(2)	173(2)
cryst syst	monoclinic	orthorhombic
space group	$P2_1/n$	$Pna2_1$
a (Å)	7.6536(6)	14.3168(10)
b (Å)	10.0022(6)	10.1697(6)
c (Å)	17.1217(15)	11.2813(10)
α (deg)	90	90
β (deg)	92.979(7)	90
γ (deg)	90	90
V (Å^3)	1308.94(17)	1642.5(2)
Z	4	4
D_{calcd} (g cm^{-3})	2.008	2.286
F(000)	768	1064
μ (mm^{-1})	7.228	10.632
cryst size (mm)	0.32 × 0.16 × 0.04	0.24 × 0.17 × 0.08
no of rflns coll	15196	10444
no of indep rflns (R_{int})	2454 (0.1068)	2878 (0.0878)
data / restr / params	2454/0/154	2878/1/181
GOOF on F^2	1.054	0.975
R_1, wR_2 ($I > 2\sigma(I)$)	0.0410, 0.0967	0.0655, 0.1408
R_1, wR_2 (all data)	0.0514, 0.1017	0.0863, 0.1491
largest diff peak and hole (e Å^{-3})	0.825 and −0.816	0.943 and −1.483

Table 2

Selected Crystallographic Data and Structure Refinement for **11** and **12**.

	11	**12**
formula	$C_{25}H_{22}Fe$	$C_{21}H_{32}BFeLiO_4$
fw	378.28	422.06
color, shape	orange, block	orange, plate
temp (K)	173(2)	173(2)
cryst syst	triclinic	orthorhombic
space group	$P\bar{1}$	*Pbcm*
a (Å)	10.6816(4)	11.476(4)
b (Å)	15.7711(6)	15.700(3)
c (Å)	17.4525(6)	12.014(3)
α (deg)	108.554(3)	90
β (deg)	93.513(3)	90
γ (deg)	97.386(3)	90
V (Å^3)	2747.74(17)	2164.6(10)
Z	6	4
D_{calcd} (g cm^{-3})	1.372	1.295
F(000)	1188	896
μ (mm^{-1})	0.828	0.719
cryst size (mm)	0.28 × 0.25 × 0.22	0.50 × 0.40 × 0.08
no of rflns coll	54170	7895
no of indep rflns (R_{int})	11837 (0.0429)	2146 (0.1071)
data / restr / params	11837/16/714	2146/0/152
GOOF on F^2	1.037	1.059
R_1, wR_2 ($I > 2\sigma(I)$)	0.0307, 0.0788	0.1261, 0.3124
R_1, wR_2 (all data)	0.0370, 0.0816	0.2103, 0.3717
largest diff peak and hole (e Å^{-3})	0.250 and −0.346	0.891 and −0.454

For Table of Contents Use Only

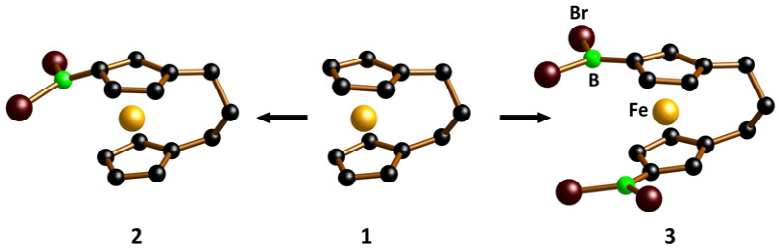

Highlights:

- The first borylated [3]ferrocenophanes have been prepared.
- In [3]Fc−BBr_2, the boryl group is bent toward the Fe center by a dip angle of 26°.
- Borylated [3]ferrocenophanes provide facile access to brominated [3]ferrocenophanes.
- Brominated [3]ferrocenophanes readily undergo Stille-type coupling reactions.
- [3]Fc−Bpin and $Li[AlH_4]$ give the unique organyl(trihydrido)borate Li[[3]Fc−BH_3].

Supporting Information

for the paper

Mono- and diborylated [3]ferrocenophanes

Adelina Reichert, Michael Bolte, Hans-Wolfram Lerner, Matthias Wagner*

Institut für Anorganische und Analytische Chemie, J.W. Goethe-Universität Frankfurt,

Max-von-Laue-Strasse 7, D-60438 Frankfurt (Main), Germany.

Corresponding author: *Matthias.Wagner@chemie.uni-frankfurt.de*

Content:

1. Syntheses of 10a, 10b, and 11.

1.1. General Considerations

Unless otherwise specified, all reactions and manipulations were carried out under dry nitrogen or argon with carefully dried and degassed solvents, flame-dried glassware, and Schlenk or glove-box techniques. Toluene and C_6D_6 were dried over Na/benzophenone and distilled prior to use. Column chromatography was performed by using silica gel 60 (Macherey–Nagel). 1D and 2D NMR spectra were recorded on Bruker AM 250, Avance 300, or Avance 400 spectrometers at room temperature. Chemical shifts are referenced to (residual) solvent signals ($^1H/^{13}C\{^1H\}$; C_6D_6: 7.15/128.0). *J* values are given in Hz. Abbreviations: s = singlet, d = doublet, dd = doublet of doublets, vt = virtual triplet, m = multiplet, n.r. = not resolved multiplet, *i* = ipso, *o* = ortho, *m* = meta, *p* = para, Cp = cyclopentadienyl, DME = 1,2-dimethoxyethane. A Biotage Initiator microwave synthesizer was used for microwave-assisted syntheses. Mass spectra were recorded with a VG PLATFORM II mass spectrometer. Combustion analyses were performed by the Microanalytical Laboratory of the Goethe-University Frankfurt. 4-Iodotoluene (Aldrich), [$PdCl_2$(dppf)] (Apollo Scientific), $^nBu_3SnPh$ (Aldrich), and [$Pd(P^tBu_3)_2$] (Apollo Scientific) are commercially available and were used as received.

*1.2. Synthesis of **10a***

Neat **6** (0.174 g, 0.494 mmol), 4-iodotoluene (0.162 g, 0.743 mmol), and [$PdCl_2$(dppf)] (0.018 g, 0.022 mmol) were charged to a Young's valve ampoule. After addition of DME (15 mL) and aqueous NaOH (3 M; 0.74 mL, 2.2 mmol), the reaction mixture was kept at reflux temperature for 6 d. $CHCl_3$ (20 mL) and H_2O (5 mL) were added and the two resulting layers were separated. The organic layer was washed with H_2O (2 × 15 mL), dried over anhydrous $MgSO_4$, filtered, and all volatiles were removed from the filtrate in vacuo. Subsequent column chromatography gave analytically pure **10a** as an orange solid. Yield: 0.051 g (33%). R_f = 0.61 (silica gel, hexane). ^1H NMR (300.0 MHz, C_6D_6): δ 7.40 (d, $^3J_{HH}$ = 8.1 Hz, 2H; Tol-H*o*), 7.00 (d, $^3J_{HH}$ = 8.1 Hz, 2H; Tol-H*m*), 4.50 (dd, $^3J_{HH}$ = 2.3 Hz, $^4J_{HH}$ = 1.5 Hz, 1H; Cp-H4), 4.34 (vt, 1H; Cp-H2), 4.16 (m, 1H; Cp-H3'/4'), 4.01 (m, 1H; Cp-H2'/5'), 3.93 (dd, $^3J_{HH}$ = 2.3 Hz, $^4J_{HH}$ = 1.5 Hz, 1H; Cp-H5), 3.72 (m,

1H; Cp-H2'/5'), 3.46 (m, 1H; Cp-H3'/4'), 2.15 (s, 3H; CH_3), 1.84–1.63 (m, 6H; CH_2); $^{13}C\{^1H\}$ NMR (75.4 MHz, C_6D_6): δ 137.2 (Tol-C*i*), 135.3 (Tol-C*p*), 129.2 (Tol-C*m*), 126.7 (Tol-C*o*), 87.1 (Cp-C3), 86.2 (Cp-C1), 85.1 (Cp-C1'), 74.4 (Cp-C3'/4'), 70.4 (Cp-C2'/5'), 70.3 (Cp-C5), 69.3 (Cp-C3'/4'), 69.1 (Cp-C2'/5'), 68.7 (Cp-C2), 67.1 (Cp-C4), 35.4 (CH_2-b), 24.9, 24.7 (CH_2-a,a'), 21.1 (CH_3). ESI-MS: *m/z* (%) = 316 $[M]^+$ (100). Anal. Calcd (%) for $C_{20}H_{20}Fe$ (316.21): C 75.96, H 6.37. Found: C 75.67, H 6.52.

*1.3. Synthesis of **10b***

A mixture of neat **8** (0.061 g, 0.20 mmol), $^nBu_3SnPh$ (0.145 g, 0.395 mmol), and $[Pd(P^tBu_3)_2]$ (0.010 g, 0.020 mmol) was dissolved in toluene (5 mL). The solution was heated in a microwave synthesizer to 170 °C for 30 min (glass vial 2–5 mL). After the reaction mixture had been cooled to room temperature, the ampoule was opened, the content was filtered, and all volatiles were removed from the filtrate in vacuo. The crude solid residue was purified by column chromatography (silica gel, hexane) to obtain **10b** as an orange solid. Yield: 0.044 g (73%). Single crystals suitable for X-ray crystallography were grown by slow evaporation of an ethanol solution of **10b** at room temperature. R_f = 0.61 (silica gel, hexane/EtOAc = 15:1). ^1H NMR (250.1 MHz, C_6D_6): δ 7.45 (m, 2H; Ph-H*o*), 7.15 (m, 2H; Ph-H*m*), 7.05 (m, 1H; Ph-H*p*), 4.48 (dd, $^3J_{HH}$ = 2.4 Hz, $^4J_{HH}$ = 1.5 Hz, 1H; Cp-H4), 4.32 (vt, 1H; Cp-H2), 4.13 (m, 1H; Cp-H3'/4'), 3.99 (m, 1H; Cp-H2'/5'), 3.93 (dd, $^3J_{HH}$ = 2.4 Hz, $^4J_{HH}$ = 1.4 Hz, 1H; Cp-H5), 3.71 (m, 1H; Cp-H2'/5'), 3.42 (m, 1H; Cp-H3'/4'), 1.84–1.61 (m, 6H; CH_2); $^{13}C\{^1H\}$ NMR (100.6 MHz, C_6D_6): δ 140.3 (Ph-C*i*), 128.5 (Ph-C*m*), 126.7 (Ph-C*o*), 126.0 (Ph-C*p*), 86.9 (Cp-C3), 86.4 (Cp-C1), 85.2 (Cp-C1'), 74.4 (Cp-C3'/4'), 70.5 (Cp-C5), 70.4 (Cp-C2'/5'), 69.3 (Cp-C3'/4'), 69.1 (Cp-C2'/5'), 68.8 (Cp-C2), 67.2 (Cp-C4), 35.4 (CH_2-b), 24.9, 24.6 (CH_2-a,a'). ESI-MS: *m/z* (%) = 302 $[M]^+$ (100). Anal. Calcd (%) for $C_{19}H_{18}Fe$ (302.18): C 75.52, H 6.00. Found: C 75.30, H 5.75.

*1.4. Synthesis of **11***

A mixture of neat **9** (0.104 g, 0.271 mmol), $^nBu_3SnPh$ (0.398 g, 1.08 mmol), and $[Pd(P^tBu_3)_2]$ (0.028 g, 0.055 mmol) was dissolved in toluene (20 mL). The solution was heated in a microwave synthesizer to 170 °C for 30 min (glass vial 10–20 mL). After the reaction mixture

had been cooled to room temperature, the ampoule was opened, the content was filtered, and all volatiles were removed from the filtrate in vacuo. The crude solid residue was purified by column chromatography (silica gel, hexane) to obtain **11** as an orange solid. Yield: 0.053 g (52%). Single crystals suitable for X-ray crystallography were grown by slow evaporation of an ethanol solution of **11** at room temperature. R_f = 0.50 (silica gel, hexane/EtOAc = 15:1). ^{1}H NMR (250.1 MHz, C_6D_6): δ 7.39 (m, 4H; Ph-H*o*), 7.15 (m, 4H; Ph-H*m*), 7.05 (m, 2H; Ph-H*p*), 4.24 (vt, 2H; Cp-H2), 4.08 (dd, $^3J_{HH}$ = 2.4 Hz, $^4J_{HH}$ = 1.4 Hz, 2H; Cp-H5), 3.91 (dd, $^3J_{HH}$ = 2.4 Hz, $^4J_{HH}$ = 1.5 Hz, 2H; Cp-H4), 1.71 (n.r., 6H; CH_2); $^{13}C\{^1H\}$ NMR (100.6 MHz, C_6D_6): δ 140.0 (Ph-C*i*), 128.5 (Ph-C*m*), 126.4 (Ph-C*o*), 126.1 (Ph-C*p*), 87.3 (Cp-C3), 86.2 (Cp-C1), 72.8 (Cp-C4), 71.5 (Cp-C5), 67.6 (Cp-C2), 35.4 (CH_2-b), 24.8 (CH_2-a). ESI-MS: *m/z* (%) = 379 $[M + H]^+$ (100). Anal. Calcd (%) for $C_{25}H_{22}Fe$ (378.28): C 79.38, H 5.86. Found: C 78.68, H 5.82.

2. Details of the X-ray Crystal Structure Analyses and Key Crystallographic Data of 6, 7, 9, and 10b.

Data for **6** and **7** were collected on a STOE IPDS II two-circle diffractometer with graphite-monochromated MoK_α radiation (λ = 0.71073 Å). An empirical absorption correction with the program PLATON [1S] was performed. Data for **9** and **10b** were collected on a STOE IPDS II two-circle diffractometer using a Genix Microfocus X-ray source with mirror optics and MoK_α radiation. The data of **9** and **10b** were corrected for absorption with the frame-scaling procedure contained in the X-AREA package. Equivalent reflections were averaged. The structures were solved by direct methods using the program SHELXS [2S], and refined with full-matrix least-squares on F^2 using the program SHELXL-97 [3S]. H atoms were geometrically positioned and refined applying a riding model.

In **7**, a methylene group is disordered over two equally occupied positions (site occupation factors 0.50(1)). The absolute structure was determined: Flack-x-parameter = 0.01(2).

Compound **9** crystallized with two crystallographically independent molecules in the asymmetric unit (**9**$^{\mathbf{A}}$, **9**$^{\mathbf{B}}$). **9** was a non-merohedral twin with a fractional contribution of 0.305(7) for the minor domain. The Fe and Br atoms of the two molecules in the asymmetric unit show pseudo-symmetry (a non-crystallographic translation of 0.5 along the c-axis). This prevents the refinement from smooth convergence. In each molecule of **9**, one methylene group is disordered over two positions with site occupation factors of 0.62(4) and 0.71(4), respectively, for the major occupied sites. The disordered atoms were isotropically refined. The displacement ellipsoid of C(14A) was restrained to an isotropic behavior to prevent it from going non-positive-definite.

Compound **10** crystallized with two crystallographically independent molecules in the asymmetric unit (**10b**$^{\mathbf{A}}$, **10b**$^{\mathbf{B}}$).

CCDC reference numbers: 926730 (**6**), 926731 (**7**), 926732 (**9**), 926733 (**10b**).

[1S] A.L. Spek, J. Appl. Crystallogr. 36 (2003) 7–13.

[2S] G.M. Sheldrick, Acta Crystallogr. A 46 (1990) 467–473.

[3S] G.M. Sheldrick, SHELXL-97, A Program for the Refinement of Crystal Structures, University of Göttingen, Göttingen, Germany, 1997.

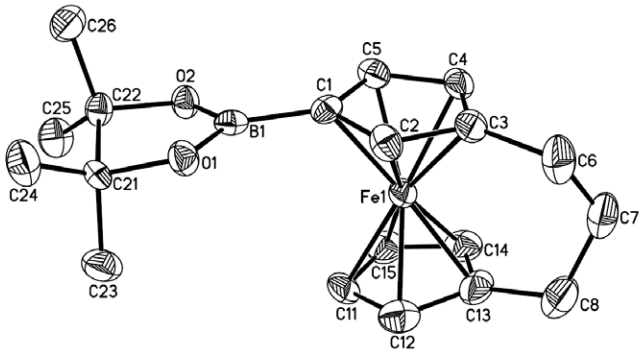

Fig. 1S. Molecular structure of **6** in the solid state. Hydrogen atoms have been omitted for clarity; displacement ellipsoids are drawn at the 50% probability level. Selected bond lengths (Å), atom···atom distance (Å), bond angles (°), and dihedral angles (°): B(1)−C(1) 1.537(7), B(1)−O(1) 1.366(7), B(1)−O(2) 1.376(7); B(1)···Fe(1) 3.139(6); C(1)−B(1)−O(1) 122.8(4), C(1)−B(1)−O(2) 123.7(5), O(1)−B(1)−O(2) 113.5(4), COG(Cp(1))−Fe(1)−COG(Cp(11)) 173.1; Cp(C(1))//Cp(C(11)) 9.7(4), B(1)O(1)O(2)//Cp(C(1)) 8.7(5), C(3)Fe(1)C(13)//C(6)C(7)C(8) 56.7(4); α* 6.0. COG(Cp(X)): centroid of the cyclopentadienyl ring containing the carbon atom C(X).

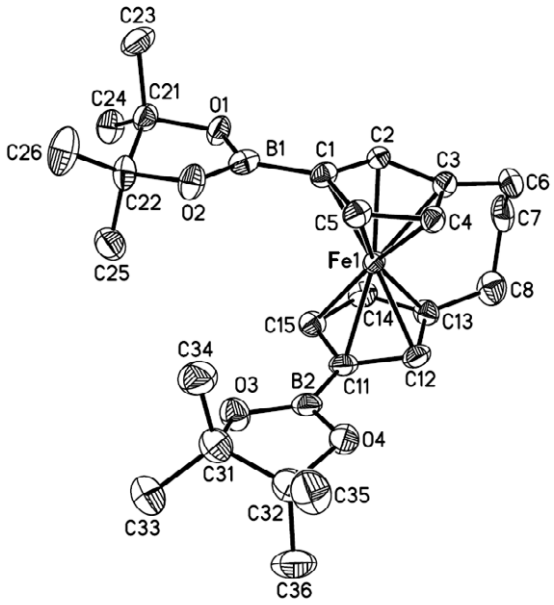

Fig. 2S. Molecular structure of **7** in the solid state. Hydrogen atoms have been omitted for clarity; displacement ellipsoids are drawn at the 50% probability level. Selected bond lengths (Å), atom···atom distances (Å), bond angles (°), torsion angle (°), and dihedral angles (°): B(1)−C(1) 1.543(6), B(2)−C(11) 1.525(6), B(1)−O(1) 1.375(5), B(1)−O(2) 1.367(5), B(2)−O(3) 1.355(5), B(2)−O(4) 1.377(5); B(1)···Fe(1) 3.182(4), B(2)···Fe(1) 3.160(5); C(1)−B(1)−O(1) 123.7(4), C(1)−B(1)−O(2) 122.6(3), C(11)−B(2)−O(3) 124.0(4), C(11)−B(2)−O(4) 122.8(4), O(1)−B(1)−O(2) 113.6(3), O(3)−B(2)−O(4) 113.1(4), COG(Cp(1))−Fe(1)−COG(Cp(11)) 171.7; C(1)−COG(Cp(1))−COG(Cp(11))−C(11) –73.8; Cp(C(1))//Cp(C(11)) 10.5(2), B(1)O(1)O(2)//Cp(C(1)) 3.9(5), B(2)O(3)O(4)//Cp(C(11)) 6.6(4), C(3)Fe(1)C(13)//C(6)C(7)C(8) 58.5(5); α* 4.1 (at C(1)), 5.0 (at C(11)).

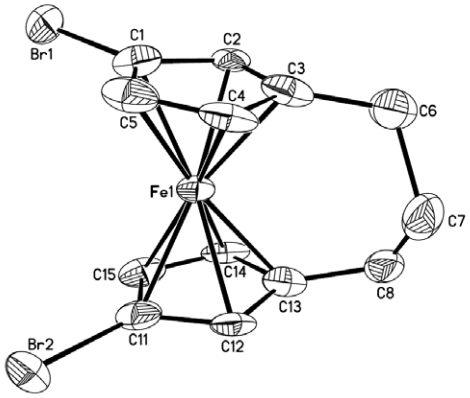

Fig. 3S. Molecular structure of $\mathbf{9^A}$ in the solid state. Hydrogen atoms have been omitted for clarity; displacement ellipsoids are drawn at the 50% probability level. The bond lengths and bond angles are not given due to poor crystallographic data, which lead to large error margins.

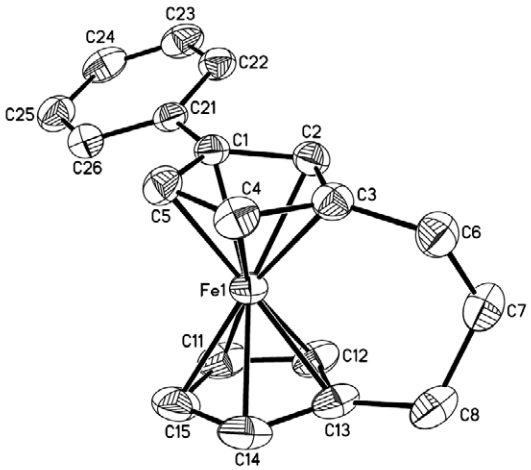

Fig. 4S. Molecular structure of $\mathbf{10b^A}$ ($\mathbf{10b^B}$) in the solid state. Hydrogen atoms have been omitted for clarity; displacement ellipsoids are drawn at the 50% probability level. Selected bond lengths (Å), bond angles (°), and dihedral angles (°): C(1)−C(21) 1.472(3) (1.471(3)); COG(Cp(1))−Fe(1)−COG(Cp(11)) 173.3 (173.3); Cp(C(1))//Cp(C(11)) 8.6(1) (8.4(2)), Cp(C(1))//Ph(C(21)) 23.4(1) (32.3(1)), C(3)Fe(1)C(13)//C(6)C(7)C(8) 58.9(2) (57.7(2)).

Table 1S

Selected Crystallographic Data and Structure Refinement for **6** and **7**.

	6	**7**
formula	$C_{19}H_{25}BFeO_2$	$C_{25}H_{36}B_2FeO_4$
fw	352.05	478.01
color, shape	yellow, plate	orange, plate
temp (K)	173(2)	173(2)
cryst syst	orthorhombic	orthorhombic
space group	*Pbca*	$Pna2_1$
a (Å)	15.0328(13)	12.6648(8)
b (Å)	10.3413(6)	11.4362(5)
c (Å)	22.7254(17)	17.3424(8)
α (deg)	90	90
β (deg)	90	90
γ (deg)	90	90
V (Å^3)	3532.9(5)	2511.8(2)
Z	8	4
D_{calcd} (g cm^{-3})	1.324	1.264
F(000)	1488	1016
μ (mm^{-1})	0.860	0.628
cryst size (mm)	0.19 × 0.15 × 0.04	0.26 × 0.18 × 0.07
no of rflns coll	17909	21304
no of indep rflns (R_{int})	3117 (0.1136)	4425 (0.0992)
data / restr / params	3117/0/208	4425/1/299
GOOF on F^2	0.907	0.927
R_1, wR_2 ($I > 2\sigma(I)$)	0.0594, 0.0915	0.0413, 0.0757
R_1, wR_2 (all data)	0.1273, 0.1090	0.0597, 0.0807
largest diff peak and hole (e Å^{-3})	0.736 and −0.491	0.215 and −0.296

Table 2S

Selected Crystallographic Data and Structure Refinement for **9** and **10b**.

	9	**10b**
formula	$C_{13}H_{12}Br_2Fe$	$C_{19}H_{18}Fe$
fw	383.90	302.18
color, shape	brown-yellow, block	brown-orange, needle
temp (K)	173(2)	173(2)
cryst syst	triclinic	monoclinic
space group	$P\bar{1}$	$P2_1/c$
a (Å)	10.1553(14)	13.9873(4)
b (Å)	11.2661(18)	22.9104(8)
c (Å)	12.7268(19)	8.7390(3)
α (deg)	63.896(11)	90
β (deg)	84.031(12)	93.997(3)
γ (deg)	72.000(12)	90
V (Å^3)	1242.7(3)	2793.64(16)
Z	4	8
D_{calcd} (g cm^{-3})	2.052	1.437
F(000)	744	1264
μ (mm^{-1})	7.612	1.065
cryst size (mm)	0.33 × 0.27 × 0.19	0.35 × 0.14 × 0.05
no of rflns coll	16308	47314
no of indep rflns (R_{int})	4365 (0.1132)	6444 (0.0864)
data / restr / params	4365/6/290	6444/0/361
GOOF on F^2	1.099	1.059
R_1, wR_2 ($I > 2\sigma(I)$)	0.1030, 0.2653	0.0401, 0.0954
R_1, wR_2 (all data)	0.1323, 0.2824	0.0491, 0.1000
largest diff peak and hole (e Å^{-3})	1.842 and −1.723	0.605 and −0.541

3. ^{1}H and $^{13}C\{^{1}H\}$ NMR Spectra of 6, 7, 8, 9, and 12.